Behavior of circular footings and plate anchors in permafrost

Ladanyi, B.; Johnston, G. H.

Publisher's version / Version de l'éditeur:

Canadian Geotechnical Journal, 11, 4, pp. 531-553, 1974-11

NATIONAL RESEARCH COUNCIL OF CANADA
CONSEIL NATIONAL DE RECHERCHES DU CANADA

BEHAVIOR OF CIRCULAR FOOTINGS AND PLATE ANCHORS IN PERMAFROST

BY

B. LADANYI AND G. H. JOHNSTON

Reprinted from
CANADIAN GEOTECHNICAL JOURNAL
Vol. 11, No. 4, November 1974
p. 531

RESEARCH PAPER NO. 618
OF THE
DIVISION OF BUILDING RESEARCH

Price 50 cents

OTTAWA

NRCC 14269

Behavior of Circular Footings and Plate Anchors Embedded in Permafrost

B. LADANYI

Department of Mining Engineering, Ecole Polytechnique, 2500 Marie-Guyard Ave., Montreal, Quebec H3C 3A7

AND

G. H. JOHNSTON

Division of Building Research, National Research Council of Canada, Ottawa, Canada K1A 0R6

Received January 4, 1974

Accepted June 3, 1974

The purpose of this paper is to develop a method for predicting the creep settlement and the bearing capacity of frozen soils under deep circular loads. The theory uses experimentally determined creep parameters of frozen soil and is intended to be applicable to the design of deep circular footings and screw anchors embedded in permafrost soils. On the basis of available experimental evidence, it was concluded that a mathematical model different from that usual in soil mechanics should be used in solving the time-dependent bearing capacity problem of such footings. The solution proposed in the paper was obtained by using the mathematical model of an expanding spherical cavity in a nonlinear viscoelastic-plastic medium with time, temperature, and normal pressure dependent strength properties. For a given footing or anchor, the theory furnishes either isochronous load-displacement curves, or load-creep rate curves, or a time-dependent bearing capacity for which formulas and graphs of nonlinear elastic-plastic bearing capacity factors are supplied.

The theoretical predictability of creep rates and ultimate failure loads was checked against the results of screw anchor tests carried out by the Division of Building Research, N.R.C.C., at a permafrost site in Thompson, Manitoba. It was found that the use in the theory of the creep parameters determined by creep-pressuremeter tests performed at the site, resulted in a satisfactory agreement between the predicted and the observed behavior.

Le but principal de cette communication est de présenter une méthode par laquelle il serait possible de prévoir le tassement dû au fluage des sols gelés et leur capacité portante lorsque sollicités par des charges circulaires profondes. Cette théorie utilise des paramètres de fluage déterminés expérimentalement. Son domaine d'application est le calcul des fondations circulaires et des ancrages établis profondement dans le pergélisol. A partir des résultats expérimentaux disponibles, on est arrivé à la conclusion que, dans la solution du problème de la capacité portante à long terme de telles fondations, il serait préférable à utiliser un modèle mathématique différent de celui habituellement en usage dans la mécanique des sols. La solution proposée dans cette communication a été obtenue à partir du modèle mathématique d'une cavité sphérique mise en expansion dans un milieu viscoélastique non linéaire plastique, dont la résistance mécanique dépend du temps, de la température et de la pression normale. Pour une fondation ou une plaque d'ancrage donnée, cette théorie fournit soit des courbes isochrones charge-déplacement, soit des courbes charge taux de fluage, soit encore la capacité portante en fonction du temps. Pour cette dernière, on a fourni des graphiques donnant des valeurs des facteurs de portance, calculés en supposant un comportement non-linéaire avant la rupture.

La possibilité de prévision théorique des taux de fluage et des charges ultimes a été vérifiée à l'aide des résultats de mise en charge de plaques d'ancrage vissées dans le pergélisol. Ces essais ont été effectués par la Division de Recherche en Bâtiment du Conseil National de Recherches du Canada sur un site près de Thompson, au Manitoba.

Cette comparaison a montré que le fait d'utiliser, dans la théorie proposée, les paramètres de fluage déterminés par des essais pressiométriques spéciaux, effectués sur le site, a permis de faire des prévisions du comportement des ancrages qui s'approchent de la réalité.

Introduction

As in other types of earth materials, the allowable pressure for a foundation or an anchor embedded deeply in frozen soil has to be determined so that the requirements for both safety against failure and admissible settlement are satisfied at any time during the service life of the structure. In unfrozen earth materials, with the exception of some particular cases that have been solved recently by numerical methods, the two requirements have usually been considered separately: The safety re-

quirement has been satisfied by substituting soil strength parameters into a Prandtl-type bearing capacity theory, and the requirement of admissible settlement has been verified by substituting soil deformation parameters into a Boussinesq-type stress-distribution theory.

Moreover, in the latter case, attention has been concentrated mainly upon the compressibility of soil which causes the major part of the settlement. The effects of temperature and of undrained (deviatoric) creep have only rarely been mentioned in connection with the determination of allowable foundation pressure in unfrozen soils, and are considered to be of secondary importance.

In frozen soils, obviously, the last two effects may become predominant in the determination of the allowable foundation pressures. It is well known that many relevant frozen soil parameters vary strongly with temperature, and that the undrained (deviatoric) creep of frozen soil contributes to the settlement of a foundation at least as much as the compression due to migration under pressure of unfrozen water and ice. Moreover, taking into account the observed behavior of frozen soil under footings and anchors, the use of a Prandtl-type bearing capacity theory is difficult to justify. It is believed, therefore, that in frozen soils an approach to allowable pressure determination different from that usual in unfrozen soils would be appropriate. It is the purpose of this paper to develop a method for predicting the creep settlement and the bearing capacity of frozen soil under deep circular loads. The theory uses experimentally determined frozen soil parameters and is intended to be applicable to the design of deep circular footings as well as circular plate and screw anchors embedded deeply in frozen soil.

Scope of the Theory

As mentioned in the introduction, the theory developed in this paper is intended mainly for calculating the time and temperature dependent settlement and rupture of deep circular footings in frozen soils. As creep is the main concern, a power law was adopted in the theory for defining the isochronous prefailure stress–strain behavior of frozen soil. Since the results so obtained are also of an isochronous type, the theory, in addition to serving the intended purpose, may, in fact, also be considered as a bearing capacity and load-settlement theory for a nonlinear elastic-plastic soil. In other words, the theory may also be used for predicting settlements and failure in ordinary soils, provided, of course, that their stress–strain behavior may approximately be defined by a power law, and that their deformation is mainly due to deviatoric strains.

Another remark concerns the footing depth. Being based on a theory of cavity expansion in an infinite medium, the solution shown in this paper is valid only when the footing behavior is essentially unaffected by the free surface. For ordinary footings, according to Meyerhof (1963), the limiting depth beyond which the effect of free surface becomes negligible is about 4 times the footing diameter for clays, and about 7–9 times the diameter for sands. An analysis of the uplift capacities of model circular footing plates in sand and clay, carried out by Meyerhof and Adams (1968), has shown that essentially the same depth limitation is valid also for deep anchor plates. It is obvious that such deep anchors, after having failed in a manner similar to deep footings, may, nevertheless, show ultimately a behavior more similar to that of shallow anchors, if the pull displacements attain large values, *e.g.* 2 or 3 times the plate diameter. This is, however, mostly considered as unacceptable in the design.

Review of Available Experimental Data

Experimental information on creep-settlement and failure of frozen soil under a loaded area is at present (1973) still very scarce and incomplete. In the Russian literature, Vialov (1959), in Chapter VII of his book, reports the results of a series of small and large scale plate loading tests in frozen soils.

In one series of tests a frozen undisturbed silty clay, in blocks of 30 × 30 × 30 cm, was loaded by circular flat ended punches with diameters of 5.05, 7.13, and 10.15 cm, respectively. The punches were placed either on the soil surface or at the bottom of a hole in the sample. In some tests the load was kept constant for long time periods (from 500 to 1600 h), while in others it was increased in steps.

In another series, a number of large scale tests were performed *in situ*, using circular plates 50.5 cm in diameter. The soil in these

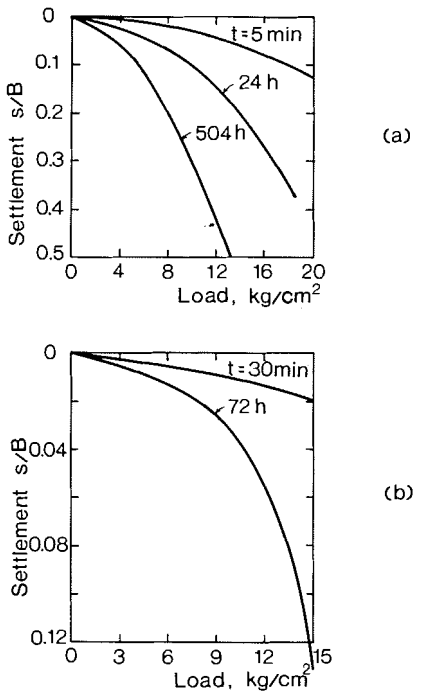

FIG. 1. Isochronous load-settlement curves from circular plate loading tests (plate diameter B = 5 cm), according to Vialov (1959).

tests was a varved clay, containing a large number of ice lenses up to 5 cm thick, with overall water content of 45%. During the tests the clay was kept at a temperature of −0.5 to −0.6 °C.

Isochronous load-settlement curves obtained in some of these tests are shown in Fig. 1(a,b). They show typical nonlinearity and time dependent behavior. Unfortunately, the curves cannot be used for any analytical purpose since no information on rheological properties of the soils involved has been given in the report. Nevertheless, it is interesting to note Vialov's observations concerning the mode of failure in these tests.

According to Vialov, the mode of failure of frozen soil under a punch is different from that of an unfrozen soil. Lateral heaving of the soil surface, usually observed, in a dense frozen soil, is absent in frozen soils, both in short term and in long term experiments, and in a large variety of soil types. A more important characteristic of the disturbance of the soil structure during penetration by a punch, is the appearance of cracks on the surface of the soil, directed radially from the axis of the punch; these were observed in many experiments with small punches in the laboratory and also in the field with punches of 50 cm diameter. In addition, as in unfrozen soils, a solid cone or 'kernel' of dense soil was formed under the flat base of the plate during penetration. This dense kernel displaced the frozen soil radially, mainly downward and laterally, with only negligible upward movement. The formation of Prandtl-type slip surfaces was not observed in these tests.

There is very little experimental information on the bearing capacity of frozen soils available elsewhere in the literature. Indirectly, however, some information obtained in deep plate anchor tests can be considered relevant to the bearing capacity in a general way. In fact, it can well be expected that within certain limits of deformation and depth of embedment, the upward movement of a deep plate anchor would result in a soil deformation similar to that occurring when the same anchor or a similar rigid structure such as a footing or a pile base, is pushed into the soil.

An extensive study of such anchors in frozen soils under long term loading was carried out between 1967 and 1970 by the Division of Building Research of the N.R.C.C. at Thompson and at Gillam, Manitoba. It is interesting to note that the results of the anchor tests and observations made during and after the tests (Johnston and Ladanyi 1974) lead to general conclusions on the soil behavior similar to those stated by Vialov for his plate load tests. In the case of plate anchors, the isochronous pressure-displacement curves were also approximately hyperbolic in shape. After excavation, no visible failure surfaces were observed around the plate but only a cone of frozen soil was found solidly attached to the plate. A typical varved clay profile after a plate anchor test is shown in Fig. 7 of the paper by Johnston and Ladanyi (1974).

Taking into account the above mentioned experimental facts, it was felt that a mathematical model different from Prandtl's and coming closer to reality should be used in considering the bearing capacity of deep footings in frozen soils. The alternative model proposed in the following is based on the theory of cavity expansion, which has often been used in similar problems.

Use of Cavity Expansion Theory in Bearing Capacity Calculations

It has been known for some time that in many materials Prandtl's theory does not represent properly the observed behavior in indentation by certain kinds of punches. Many observations show that under certain conditions, which are mainly a function of the material properties and the punch geometry, instead of producing lateral shear failure as assumed by Prandtl, the punch indentation results only in a general elastic-plastic deformation of the indented material. In other words, the indentation creates a plastic nucleus which, even after unloading, keeps the surrounding elastic mass in equilibrium and prevents the hole from closing.

A complete solution of an elastic-plastic indentation problem is rather complex even for relatively simple assumptions on the material behavior. Until now, it has not been possible to solve it explicitly, but some particular cases have been solved by numerical methods (Duncan and Chang 1970; Girijavallabhan and Reese 1968).

Although it may be interesting to solve some important particular practical cases by numerical methods, one can hardly afford to do so in ordinary engineering practice where, in most cases, only 'order of magnitude' solutions are sufficient and where many factors are known only approximately. At present, therefore, there may be some justification in looking for simpler mathematical models which, while not giving an accurate solution of a particular problem, enable one to visualize quite closely its most important features. In deep indentation problems such a close approximation to the true solution is given by the theory of cavity expansion. The expansion theory was first used for that purpose by Bishop *et al.* (1945) in connection with deep punching of metals. It has since been used with success by different authors and for various types of materials, *e.g.* Dugdale (1958) and Mulhearn (1959) for metals, Marsh (1964) for glass, Gibson (1950) for clays, Skempton *et al.* (1953) for sands, and Ladanyi (1959) for sands, for sensitive clays (1967*a*) and for rocks (1966, 1967*b*).

Some recent work by Hirst and Howse (1969) and by Johnson (1970) shows clearly the dependence of material response to indentation on the material properties and the punch geometry. In particular, for a variety of materials, it is found that, for a given punch geometry, the type of response depends mainly on the value of the E/Y ratio, where E is Young's modulus, and Y is the yield point in simple compression. Since E/Y is equal to the reciprocal value of the yield strain, low E/Y values imply very deformable materials, while high E/Y values correspond to rigid materials. According to Hirst and Howse (1969), four main types of deformation can be observed for indentation of real materials by hard wedges. Figure 2 indicates the regions of E/Y and the wedge angle in which they may be expected to occur.

Figure 2 shows that plastic rigid type of failure may be expected only in materials of low deformability when penetrated by sharper wedges. For blunt wedges (wedge angle $\approx 180°$), and materials of medium E/Y ratios, (*i.e.* $50 < E/Y < 1000$), cavity expansion seems to be the closest simple mathematical model. Since this is exactly the region of E/Y valid for most cohesive unfrozen, and frozen soils, the use of the theory of cavity expansion as a proper mathematical model for penetration problems is well indicated. In comparison with Prandtl's theory which takes into account only the failure characteristics of the material, the cavity expansion theory enables one to consider easily the whole stress–strain behavior and its time and temperature dependence. Furthermore, it is a convenient method for predicting not only the failure loads but also a large part of the plastic settlement curve.

Transformation of Cavity Expansion Results to Deep Punching Data

The theory of cavity expansion owes its great versatility to the fact that it considers a highly symmetric problem, thus permitting relatively simple analytical solutions to be obtained, even for a rather complex material behavior. When used for a less symmetric case, such as the deep punching problem, it is obvious that it represents only one part of the solution, and, therefore, some additional assumptions are required. From observations made in deep punching of metals, Bishop *et al.* (1945) and Hill (1950) conclude that the pressure required to produce a deep hole in an elastic-plastic medium is proportional to that

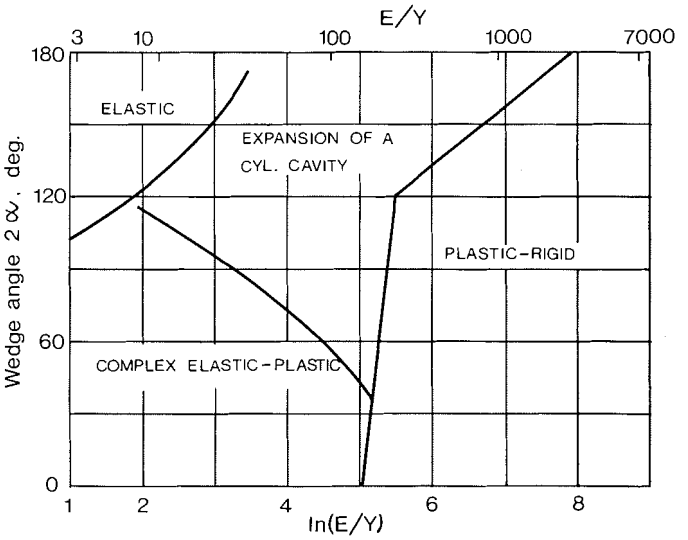

FIG. 2. Regions of operation of the different wedge indentation mechanisms, according to Hirst and Howse (1969).

necessary to expand a cavity of the same volume and under the same conditions, provided there is no friction present.

In soil mechanics, the transformation from a cavity expansion solution to a punching problem has usually been made by assuming, as proposed by Gibson (1950) that during the penetration of the punch a rigid cone (or wedge) of soil is formed at the base of the punch, the lateral surface of which is acted upon by a uniformly distributed soil pressure whose normal component is equal to the cavity expansion pressure, p_i (Fig. 3).

At failure, the shear strength of the soil over the whole area of the cone is assumed to be fully mobilized. From statical considerations it is found, both for a cone and for a wedge, that the following relationship holds

$$[1] \quad q_{as} + H = (p_{ias} + H)(1 + \tan \phi \cot \alpha)$$

where: q_{as} denotes the average pressure acting on the punch at failure, p_{ias} is the asymptotic value of the cavity expansion pressure acting normally upon the cone (or wedge) with the semi angle α at the tip, ϕ is the angle of internal friction of the soil, and

$$[2] \quad H = c \cot \phi$$

in which c is the time and temperature dependent cohesion of frozen soil.

For a circular, flat-ended punch, both theory

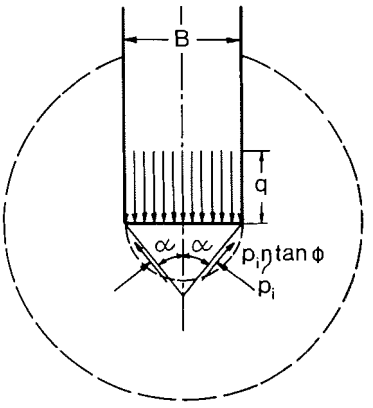

FIG. 3. Schema for transformation of a cavity expansion to a deep punching problem.

and experiments, (Berezantsev 1956; De Beer and Ladanyi 1961) show that α is very close to 45°, enabling, for practical purposes, Eq. [1] to be written as

$$[3] \quad q_{as} \approx p_{ias}(1 + \tan \phi) + c$$

During the prefailure period, it may be expected that the relationship between the punching pressure and the cavity expansion pressure will also depend upon the existence of the cone and the degree of the shear strength mobilization over the conical surface. Clearly, since both of these depend upon the specific displacement of the punch, the relationship

between the two pressures may be written in the form

$$[4] \quad q + H = (p_i + H)[1 + \eta \tan \phi \cot \alpha]$$

where: q is the applied punching pressure, p_i is the corresponding cavity expansion pressure, and η is a dimensionless coefficient expressing the degree of mobilization of shear strength on the cone for a given specific settlement. Based upon the results of some recent deep plate-loading tests on stiff clays (Burland *et al.* 1966), which are similar to stiff frozen soils, it appears that the ultimate load is attained at a settlement of about one-tenth of the plate diameter. It is therefore proposed, as a first approximation, to define η as:

$$\eta = 10s/B \quad \text{if } s < 0.1B$$

and

$$\eta = 1 \quad \text{if } s \geq 0.1B$$

where B is the punch diameter and s is the total settlement.

For frictionless materials, Eqs. [1] and [4] reduce to

$$[5] \quad q_{as} = p_{ias} + c \cot \alpha$$

and

$$[6] \quad q = p_i + \eta c \cot \alpha$$

For penetrations smaller than about one-half of punch diameter, the amount of punch penetration can be evaluated approximately from the cavity expansion displacements by equalizing the displaced volumes in both cases (Johnson 1970; Ladanyi 1966).

A settlement s of a circular punch results in a volume displacement of

$$[7] \quad V_s = \pi r_{io}^2 s$$

where $r_{io} = B/2$ is the radius of the punch. On the other hand, the original volume of the hemisphere to be expanded by the punch penetration is

$$[8] \quad V_{io} = \frac{2}{3}\pi r_{io}^2$$

if the hemisphere is assumed to have originally the same diameter as the punch. The punch penetration s is assumed to expand the hemisphere by V_s, so that, after expansion

$$[9] \quad V_i = V_{io} + V_s$$

from which

$$[10] \quad \frac{V_i}{V_{io}} = 1 + \frac{3}{2}\left(\frac{s}{r_{io}}\right) = 1 + 3\frac{s}{B}$$

Since the theory of cavity expansion furnishes a relationship between p_i and V_i/V_{io}, Eqs. [4] and [10] allow the corresponding pressure-penetration relationship to be estimated from the former.

Assumptions on the Frozen Soil Behavior

A. $\phi = 0$ Material (Fig. 4A)

Behavior in Prefailure State

It has been shown in a previous paper (Ladanyi 1972), that, for an axially symmetric case, a convenient way of expressing the axial steady state creep rate of a frozen soil, taking into account the effect of temperature is by writing

$$[11] \quad \dot{\epsilon}_1^{(c)} = \dot{\epsilon}_c \left(\frac{\sigma_1 - \sigma_3}{\sigma_{cuo} f(\theta)}\right)^n$$

where: $\dot{\epsilon}_c$ is an arbitrary creep rate, σ_{cuo} is the creep proof stress in uniaxial compression extrapolated to 0 °C, $n \geq 1$ is the creep exponent, and $f(\theta)$ is a temperature function which may take various forms, such as exponential, power, or even linear, for small temperature variations (Ladanyi 1972; Johnston and Ladanyi 1972). For brevity, Eq. [11] can be written as

$$[12] \quad \dot{\epsilon}_1^{(c)} = \left(\frac{\sigma_1 - \sigma_3}{\bar{\sigma}_c}\right)^n$$

where

$$[13] \quad \bar{\sigma}_c = \sigma_{cuo} f(\theta) \dot{\epsilon}_c^{-1/n}$$

For constant loading and temperature conditions, Eq. [11] can be integrated to give an isochronous stress–strain curve valid for a constant time interval t. Experimental evidence shows that for intervals longer than about 24 h, the instantaneous portion of strain becomes less than about 10% of the total, so that it can be neglected (Vialov 1959). The total strain is then given approximately by (Eq. [14] in Ladanyi 1972):

$$[14] \quad \epsilon_1 \approx \epsilon_1^{(c)} = \dot{\epsilon}_c t \left[\frac{\sigma_1 - \sigma_3}{\sigma_{cuo} f(\theta)}\right]^n$$

for brevity, Eq. [14] can be written as

$$[15] \quad \epsilon_1 = \left(\frac{\sigma_1 - \sigma_3}{\sigma_s}\right)^n$$

where

$$[16] \quad \sigma_s = \sigma_{cuo} f(\theta)[\dot{\epsilon}_c t]^{-1/n}$$

Behavior in Failure State

It is assumed that the frictionless frozen

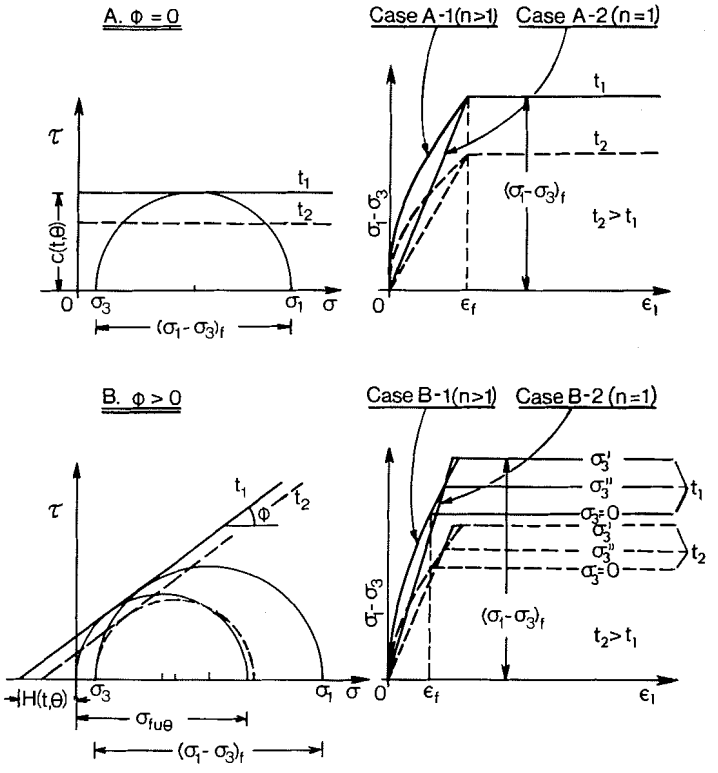

FIG. 4. Basic assumptions on frozen soil behavior used in the theory.

soil fails according to the von Mises criterion, which, for an axially symmetric case, (with $\sigma_1 > \sigma_2 = \sigma_3$), reduces to

$$[17] \qquad \sigma_1 - \sigma_3 = \sigma_{fu}$$

where σ_1 and σ_3 are the major and the minor principal stresses, respectively, and σ_{fu} is the time and temperature dependent uniaxial strength, equal to twice the soil mechanics cohesion, c:

$$[18] \qquad \sigma_{fu}(t, \theta) = 2c(t, \theta)$$

The value of σ_{fu} can be expressed in terms of time and temperature, according to Eq. [65] in Ladanyi (1972), by

$$[19] \quad \sigma_{fu}(t, \theta) = \sigma_{cuo} f(\theta) \left(\frac{\epsilon_f}{t\dot{\epsilon}_c}\right)^{1/n} = \sigma_{cu\theta} \left(\frac{\epsilon_f}{t\dot{\epsilon}_c}\right)^{1/n} = \bar{\sigma}_c \left(\frac{\epsilon_f}{t}\right)^{1/n}$$

where ϵ_f denotes a constant average creep failure strain, while t is the selected time parameter, *e.g.* the service life of the structure.

B. $\phi > 0$ Material (Fig. 4B)

Behavior in Prefailure State

As shown in Ladanyi (1972), a convenient empirical expression for describing the creep from the unstressed state of a frozen frictional soil obeying the Mohr-Coulomb failure criterion, is

$$[20] \qquad \dot{\epsilon}^{(c)} = \dot{\epsilon}_c \left(\frac{\sigma_1 - \sigma_3}{\sigma_{cu\theta} + \sigma_3(f_c - 1)}\right)^n$$

where f_c is the flow value given by

$$[21] \qquad f_c = \frac{1 + \sin \phi_c}{1 - \sin \phi_c}$$

in which ϕ_c denotes the slope of the Coulomb failure envelope corresponding to the strain rate $\dot{\epsilon}^{(c)} = \dot{\epsilon}_c$. All other symbols are defined as in Eq. [11].

As in the $\phi = 0$ case, one could combine Eq. [20] with a creep rupture condition to obtain a solution of the cavity expansion problem. Although this is not a very difficult mathematical exercise, it has been found that the

solution so obtained is too complicated for practical use. Moreover, as can be seen from the test results for a frozen sand–ice mixture reported by Andersland and Alnoury (1970), Sayles (1973), and Alkire and Andersland (1973), doubling or even tripling the value of σ_3 did not have a marked effect on the shape of the prefailure portion of the stress–strain curves, if the sample seating effect is excluded.

For the sake of simplicity it has been decided, therefore, to neglect the effect of the confining pressure on the creep rate in the prefailure state in the following analysis, *i.e.* to use Eq. [11] instead of Eq. [20] for describing the steady state creep rate. This is analogous to adopting, in an ordinary linear-elastic case, a constant average value of the deformation modulus, instead of its true value which varies with pressure. This simplifying assumption is quite often made when solving engineering problems in soil and rock mechanics.

Consequently, the constitutive equations adopted in the following analysis for describing the behavior of a frictional frozen soil are in prefailure state (Eqs. [15] and [16]):

$$\epsilon = \left(\frac{\sigma_1 - \sigma_3}{\sigma_{sa}}\right)^n \qquad [22]$$

where

$$\sigma_{sa} = \sigma_{cao} f(\theta)[\dot{\epsilon}_c t]^{-1/n} \qquad [23]$$

is an average σ_s value corresponding to an average creep proof stress σ_{cao} which is not a result of a series of unconfined creep tests as σ_{cuo}, but of a series of confined creep tests obtained at an average confining pressure σ_{3av}, representative of the range to be expected in the problem under consideration.

Behavior in Failure State

It is assumed that the frictional frozen soil fails according to the extended Coulomb–Mohr criterion which, for an axially symmetric case, reduces to

$$\frac{\sigma_{max} + H}{\sigma_{min} + H} = f \qquad [24]$$

where σ_{max} and σ_{min} are the major and the minor principal stress, respectively, f is the flow value given by Eq. [21] and

$$H(t, \theta) = c(t, \theta) \cot \phi \qquad [25]$$

with

$$c(t, \theta) = \sigma_{fu}(t, \theta)/2\sqrt{f} \qquad [26]$$

where $\sigma_{fu}(t, \theta)$ is given by Eq. [19] as before. The creep strain ϵ_f in Eq. [19] refers now only to the unconfined state. For confining pressures different from zero, this formulation implies that ϵ_f will increase with an increasing σ_3, as shown in Fig. 4B. This is in agreement with the available experimental data on the behavior of saturated frozen sands in triaxial compression (Sayles 1973; Alkire and Andersland 1973).

Proposed Method of Solution

A number of methods of solution are available at present that can be applied to solving a cavity expansion problem in materials with time dependent properties. The choice of a proper method depends on the properties of the material, as well as on the character and the required accuracy of the expected answer.

If the material has a linear viscoelastic behavior, the problem can be solved conveniently by using the Laplace transform method (*e.g.* Gill 1970). If, on the other hand, the material has a nonlinear viscoelastic behavior, steady state creep solutions can be obtained for a given steady state creep law by using the 'Hoff's analogue' (Hoff 1954) enabling a nonlinear creep problem to be reduced to a nonlinear elasticity problem.

If, in addition to being nonlinear viscoelastic, the material behavior is also affected by its time and pressure dependent strength properties, as is the case with the frozen soil, not many direct solution procedures are applicable.

A procedure, which is not direct, but is relatively simple, consists in expressing the deformation and strength properties of frozen soil as functions of time and temperature. Once the range of load, time, and temperature relevant to the problem has been decided upon, the problem can be solved as an ordinary nonlinear elastic-plastic problem on the basis of time and temperature dependent stress–strain and strength properties.

Obviously, since such a solution is based upon isochronous stress–strain curves, which are not the true stress–strain curves valid for a monotonous loading but are deduced from constant-stress creep curves, the resulting load-displacement relationship will also be of an isochronous type. Consequently, such a solution can be used directly only for finding the amount of creep settlement of a deep footing under a

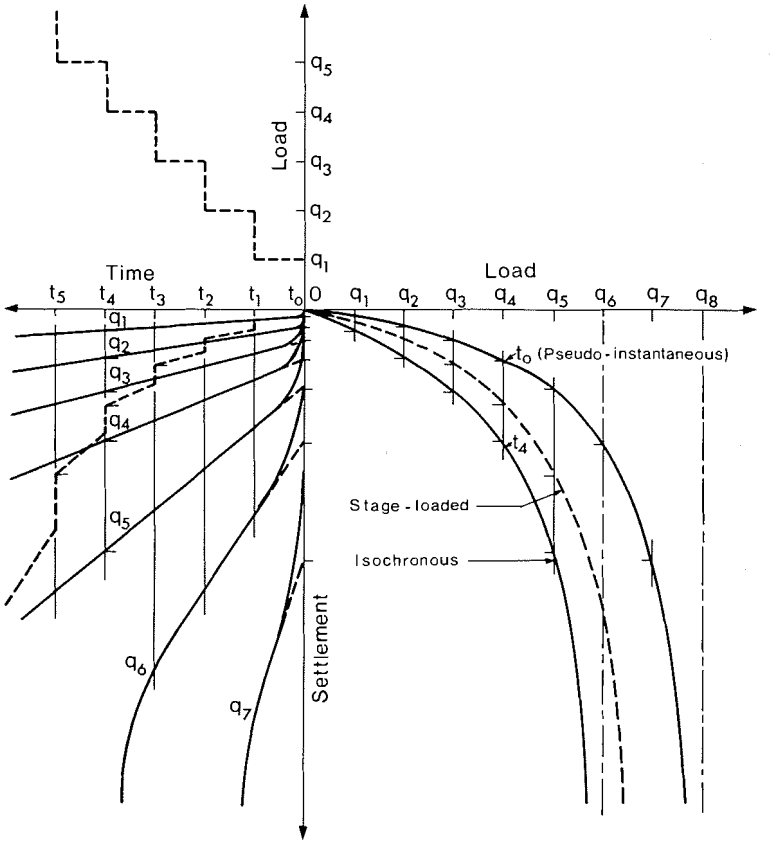

FIG. 5. Schematic presentation of the load-settlement-time relationship in loading tests.

step-load and at a given freezing temperature. On the other hand, for a series of step-wise load increments and temperature variations, an approximate answer can be obtained by superposition, as shown in Fig. 5.

Nevertheless, for a nonlinear creep range without failure, as well as for the whole range of creep and failure in a $\phi = 0$ material, it can be shown that the Hoff's analogue remains valid. In that case it is therefore possible to determine analytically the rate of cavity expansion under a constant internal pressure, which is directly related to the rate of settlement of the deep footing under a step load.

In all the cases solved in the following a common assumption is made that the medium is originally homogeneous and isotropic and subjected to an isotropic stress tensor p_0.

As far as failure is concerned, two separate solutions are shown, one for a $\phi = 0$ material and another for a $\phi > 0$ material both following a Mohr–Coulomb formulation of the failure condition. The former is intended to cover the cases of very ice-rich soils, frozen clays, peat, and pure ice. The latter, in turn, corresponds to frozen dense sands, silts, and gravels. All the materials are assumed to be saturated with ice so that volume compression strains can be neglected in the calculation.

When the two types of materials are combined with a nonlinear and a linear prefailure behavior, respectively, four different cases are obtained, for which the formulae for calculating creep displacements and failure loads are developed in the following. Subsequently, a recapitulation of the most important expressions for the two nonlinear cases is presented, in order to facilitate the use of the theory in the design.

Theory

In the development of the theory, the usual procedure has been followed: First, the stresses and displacements in each separate region

around the cavity have been found. Then, by satisfying the continuity and the boundary conditions, the relationship between the pressure p_i in the cavity and the corresponding radial displacements or displacement rate of the cavity wall has been determined.

A. Solution for a $\phi = 0$ Material

Case (A-1): Nonlinear Creep Behavior

Stresses and displacements in prefailure region ($r_e < r < \infty$). In a spherical region around the cavity extending from a radius $r_e \geq r_i$ to infinity (Fig. 6), the material is assumed to be in prefailure state, behaving according to Eq. [15]. Moreover, owing to the adopted general assumptions, the conditions of equilibrium reduce to only one differential equation

$$[27] \qquad \frac{d\sigma_r}{dr} + 2\frac{\sigma_r - \sigma_t}{r} = 0$$

where σ_r is the major principal stress (radial) and σ_t is the minor principal stress (circumferential).

For an incompressible material with a nonlinear stress–strain defined by Eq. [15], the solution can readily be found, and has been quoted in several textbooks (Odquist and Hult 1962; Hult 1966). According to this solution, the stresses in the prefailure region are

$$[28] \qquad \sigma_r = (\sigma_{re} - p_o)\left(\frac{r_e}{r}\right)^{3/n} + p_o$$

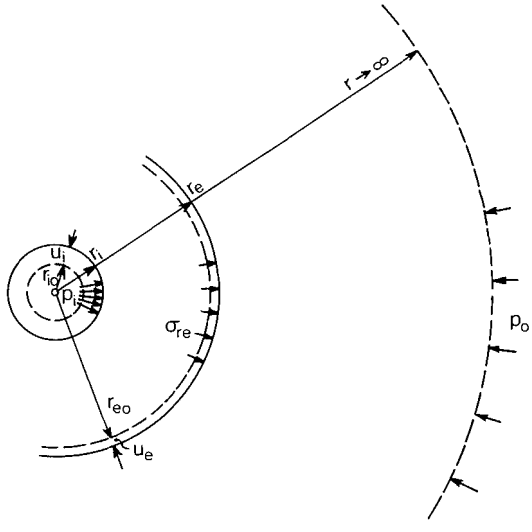

FIG. 6. Notation in cavity expansion theory.

$$[29] \qquad \sigma_t = (\sigma_{re} - p_o)\left(1 - \frac{3}{2n}\right)\left(\frac{r_e}{r}\right)^{3/n} + p_o$$

where σ_{re} denotes the radial stress at $r = r_e$ (Fig. 6).

It will be seen that for $n = 1$ the two equations reduce to the well known Lamés equations for expansion of a spherical cavity in a linear-elastic medium.

The corresponding displacement field is defined by

$$[30] \qquad \frac{u}{r} = \frac{1}{2}\left[\frac{3(\sigma_{re} - p_o)}{2n\sigma_s}\right]^n\left(\frac{r_e}{r}\right)^3$$

where u is the radial displacement at a distance r from the center of the cavity.

Failure Region ($r_i < r < r_e$). Substituting the failure condition, Eq. [17], into the equilibrium Eq. [27], integrating, and considering the boundary condition $\sigma_r = p_i$ at $r = r_i$, one gets the well known equations for the stresses in the failure region

$$[31] \qquad \sigma_r = p_i - 4c\ln\frac{r}{r_i}$$

$$[32] \qquad \sigma_t = p_i - 2c\left(1 + 2\ln\frac{r}{r_i}\right)$$

The extent of the failure region can be obtained from the continuity of the stresses at the interface between the two regions. For $r = r_e$, Eqs. [28], [29], [31], and [32] give

$$[33] \qquad \sigma_{re} = p_i - 4c\ln\frac{r_e}{r_i}$$

$$[34] \qquad \sigma_{te} = \left(1 - \frac{3}{2n}\right)(\sigma_{re} - p_o) + p_o = p_i - 2c\left(1 + 2\ln\frac{r_e}{r_i}\right)$$

Eliminating σ_{re} one gets

$$[35] \qquad \ln\frac{r_e}{r_i} = \frac{p_i - p_o}{4c} - \frac{n}{3}$$

From Eqs. [33] and [35],

$$[36] \qquad \sigma_{re} - p_o = \frac{4}{3}cn$$

which, substituted into Eq. [30], gives the displacement at $r = r_e$,

$$[37] \qquad \frac{u_e}{r_e} = \frac{1}{2}\left(\frac{2c}{\sigma_s}\right)^n$$

A complete displacement field in the failure zone can be obtained by the methods of incremental plasticity, as shown by Hill (1950). However, if only the pressure-expansion curve has to be determined, it is sufficient to know only the radial displacements at the boundaries of the region. A satisfactory answer to this problem can be obtained from geometrical considerations, and by introducing the idea of an average total volume strain in the failure region, e_{av}, positive for compression (Ladanyi 1963).

From the geometry of Fig. 6, by equating the volumes of the failure zone before and after the displacement u_i of the inner boundary, and after neglecting certain small magnitudes of higher order, the following expression can be deduced

$$[38] \quad \frac{V_i}{V_{io}} \equiv \left(1 + \frac{u_i}{r_{io}}\right)^3 \equiv \left(1 - \frac{u_i}{r_i}\right)^{-3} = \frac{1 - e_{av}}{1 - A_s}$$

where V_i and V_{io} denote the current and the initial volume of the cavity, respectively, r_i and r_{io} the corresponding radii, u_i the radial displacement of the cavity wall, while A_s is defined by

$$[39] \quad A_s = \left(\frac{r_e}{r_i}\right)^3 \left(3\frac{u_e}{r_e} + e_{av}\right)$$

Substituting Eqs. [35] and [37] into Eq. [39], one gets

$$[40] \quad A_s = \left[e_{av} + \frac{3}{2}\left(\frac{2c}{\sigma_s}\right)^n\right] \times \exp\left[\frac{3(p_i - p_o)}{4c} - n\right]$$

Since the $\phi = 0$ condition usually characterizes a frozen saturated clay or a frozen sand with high ice content, the average volume strain in the failure region, e_{av}, is expected to be very small and can be neglected. When A_s from Eq. [40] is substituted into Eq. [38], one gets the equation of an isochronous and isothermal pressure-expansion curve of a general form $V_i/V_{io} = f(p_i - p_o)$. This curve is valid from the moment the frozen soil starts to fail around the cavity, up to the general expansion failure of the medium. As seen from Eq. [38], this latter event can be expected to occur only asymptotically when A_s tends to unity. The asymptotic value of the expansion pressure, p_{ias}, is then equal to

$$[41] \quad p_{ias} = p_o + \frac{4}{3}c\left[n + \ln\frac{2}{3}\left(\frac{\sigma_s}{2c}\right)^n\right]$$

Eq. [41] can also be written as

$$[42] \quad p_{ias} = p_o N_p + cN_{pc}$$

with

$$N_p = 1$$

and

$$[43] \quad N_{pc} = \frac{4}{3}\left[n + \ln\frac{2}{3}\left(\frac{\sigma_s}{2c}\right)^n\right]$$

or, owing to Eqs. [16], [18], and [19],

$$[44] \quad N_{pc} = \frac{4}{3}\left[n + \ln\frac{2}{3\epsilon_f}\right]$$

Similarly, using Eq. [5] (with $\cot\alpha = 1$), one can get from Eq. [42] the corresponding asymptotic punching pressure, q_{as}

$$[45] \quad q_{as} = p_o N_q + cN_c$$

with

$$N_q = 1$$

and

$$[46] \quad N_c = N_{pc} + 1 = 1 + \frac{4}{3}\left[n + \ln\frac{2}{3\epsilon_f}\right]$$

In Fig. 7 the variation of factor N_c, Eq. [46], is shown for n varying from 1 to 10, and for five different values of the failure strain ϵ_f or the ratio $(2c/\sigma_s)^n$. For $n = 1$, the values of N_c reduce to those valid for an incompressible linear elastic perfectly plastic material.

Pressure-settlement Behavior. For calculating the whole isochronous settlement curve, one may proceed as follows: When failure region exists, which, according to Eq. [35] occurs only when

$$[47] \quad p_i - p_o > \frac{4}{3}nc$$

or, due to Eq. [6], (with $\alpha = 45°$), when

$$[48] \quad q - p_o > c\left(\frac{4}{3}n + \eta\right)$$

or, with Eq. [42], when

$$[49] \quad q_{as} - q < c\left[N_c - \frac{4n}{3} - \eta\right],$$

Eqs. [38] and [40] are valid. They give for $A_s \neq 1$ and $A_s = 1$, respectively,

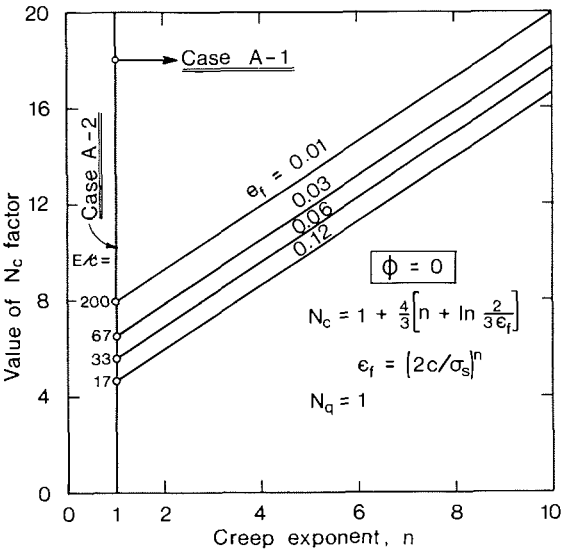

FIG. 7. Values of bearing capacity factor N_c for $\phi = 0$, and for linear (case A-2) and nonlinear (case A-1) creep.

$$[50] \quad 1 - \frac{1}{V_i/V_{io}} = \frac{3}{2}\left(\frac{2c}{\sigma_s}\right)^n \times \exp\left[\frac{3(p_i - p_o)}{4c} - n\right]$$

and

$$[51] \quad 1 = \frac{3}{2}\left(\frac{2c}{\sigma_s}\right)^n \exp\left[\frac{3(p_{ias} - p_o)}{4c} - n\right]$$

Dividing Eq. [51] by Eq. [50], one gets

$$[52] \quad \frac{V_i}{V_{io}} = \left[1 - \exp\left(-\frac{3}{4c}\right)(p_{ias} - p_i)\right]^{-1}$$

Further, using Eqs. [10], [5], and [6], one gets for the isochronous settlement curve:

$$[53] \quad \frac{s}{B} = \frac{1}{3}\left(\frac{V_i}{V_{io}} - 1\right) = \frac{1}{3}\left\{\left[1 - \exp\frac{3}{4}\left(\frac{q - q_{as}}{c} + 1 - \eta\right)\right]^{-1} - 1\right\}$$

or, with Eq. (45)

$$[54] \quad \frac{s}{B} = \frac{1}{3}\left\{\left[1 - \exp\frac{3}{4}\left(\frac{q - p_o}{c} + 1 - \eta - N_c\right)\right]^{-1} - 1\right\}$$

If the failure zone does not exist yet, which happens according to Eq. [48] when

$$[55] \quad q - p_o < c\left(\frac{4n}{3} + \eta\right)$$

the pressure-settlement curve is given according to Eqs. [10] and [38] by

$$[56] \quad \frac{s}{B} = \frac{1}{3}\left[\left(1 - \frac{u_i}{r_i}\right)^{-3} - 1\right]$$

in which u_i/r_i is obtained by setting in Eq. [30] $\sigma_{re} = p_i$ and $r_e = r = r_i$. Equation [56] becomes then

$$[57] \quad \frac{s}{B} = \frac{1}{3}\left\{\left[1 - \frac{1}{2}\left(\frac{3(p_i - p_o)}{2n\sigma_s}\right)^n\right]^{-3} - 1\right\}$$

Or, taking into account Eqs. [6] and [16] to [19],

$$[58] \quad \frac{s}{B} = \frac{1}{3}\left\{\left[1 - \frac{\epsilon_f}{2}\left(\frac{3(q - p_o - \eta_c)}{4nc}\right)^n\right]^{-3} - 1\right\}$$

The ambient pressure p_o in all settlement formulae should be considered as the average original normal pressure at the level of the punch. For example, assuming equality of horizontal principal stresses

$$[59] \quad p_o = \frac{1}{3}p_v(1 + 2K_o)$$

in which p_v is the total vertical pressure and K_o is the at rest earth pressure coefficient. No field information is available as yet on the value of K_o in frozen soil layers, but intuitively one can expect it to be larger than in the same soil when unfrozen, because of residual lateral stresses generated during freezing.

As a first approximation, one may take, therefore, $K_o = 1$, *i.e.* $p_o = p_v$, but lower values are also possible in the region of vertical thermal cracks.

Equations [53] and [58] give the amount of creep settlement of a deep circular punch embedded in frozen soil of constant temperature θ, if a step load q is applied and maintained constant during a time interval t. Obviously, by varying t, one can find the whole development of settlement with time. Inversely, noting that in Eqs. [45], [54], and [58] c is a function of time, given by Eqs. [18] and [19], one can also deduce from the same equations the time necessary for a given settlement to be attained under a constant load q. In particular, from Eq. [45]

it follows that the time to failure (infinite settlement) under a load q, satisfying the inequality Eq. [48], will be

$$[60] \quad t_f = \epsilon_f \left[\frac{\bar{\sigma}_c N_c}{2(q - p_o)}\right]^n = \frac{\epsilon_f}{\dot{\epsilon}_c}\left[\frac{\sigma_{cu\theta} N_c}{2(q - p_o)}\right]^n$$

Creep Rate by the Hoff's Analogue. In order to find the steady state creep solution by the Hoff's elastic analogue method, it is sufficient to replace the stress–strain law, Eq. [15], by the corresponding creep law, Eq. [11], and all strains and displacements by their derivatives with respect to time. It is well known that the steady state creep stresses then remain equal to the stresses in the corresponding nonlinear elastic solution. Equations [28] and [29] remain valid, therefore, during the steady state creep. The radial displacement rate of the cavity wall in pre-failure stage thus becomes, according to Eq. [30]:

$$[61] \quad \frac{\dot{u}_i}{r_i} = \frac{1}{2}\left[\frac{3(p_i - p_o)}{2n\bar{\sigma}_c}\right]^n = \frac{\dot{\epsilon}_c}{2}\left[\frac{p_i - p_o}{2n\sigma_{cu\theta}/3}\right]^n$$

and the corresponding settlement rate, $\dot{s}/B$, is obtained by substituting $\dot{u}_i/r_i$ into Eq. [56] instead of u_i/r_i. When the failure region exists, the settlement rate can only be obtained indirectly from Eq. [54], by observing that c is a function of time defined by Eqs. [18] and [19] as

$$[62] \quad c = \frac{1}{2}\bar{\sigma}_c(\epsilon_f/t)^{1/n}$$

Case (A-2): Linear Creep Behavior

This case is, in fact, a special case of the foregoing nonlinear elastic plastic ($\phi = 0$) case. In order to transform the former solution into a corresponding solution for the linear case, it is sufficient to put $n = 1$ in all expressions and to replace σ_s by the (time and temperature dependent) modulus of elasticity E. One thus obtains the classical linear-elastic perfectly plastic solution for the expansion of a spherical cavity in an incompressible medium (Bishop *et al.* 1945; Hill 1950).

If, on the other hand, it is assumed, as in Bishop *et al.* (1945), that the material is compressible ($\nu \neq 0.5$) in prefailure state only, one gets for N_{pc} instead of Eq. [43],

$$[63] \quad N_{pc} = \frac{4}{3}\left[1 + \ln\frac{E}{2(1 + \nu)c}\right]$$

Another expression affected by the Poisson's ratio is Eq. [40] which, for $\nu \neq 0.5$, becomes

$$[64] \quad A_s = 2\frac{(1 + \nu)c}{E}\exp\left[\frac{3(p_i - p_o)}{4c} - 1\right]$$

Equations [52]–[54] remain unchanged. In the prefailure period of cavity expansion one gets instead of Eq. [57] a settlement formula based on Lamé's theory:

$$[65] \quad \frac{s}{B} = \frac{1}{3}\left\{\left[1 - \frac{1 + \nu}{2E}(q - p_o - \eta c)\right]^{-3} - 1\right\}$$

It is interesting to compare Eq. [65] with the analogous Boussinesq equation for the settlement of a rigid circular load on the surface of an elastic solid

$$[66] \quad \frac{s}{B} = \frac{\pi}{4}(1 - \nu^2)\frac{q}{E}$$

At the surface $p_o \approx 0$, and for small strains, ($\eta = 0$), Eq. [65] becomes

$$[67] \quad \frac{s}{B} \approx \left(\frac{1 + \nu}{2}\right)\frac{q}{E}$$

Comparing Eq. [66] with Eq. [67] leads to the conclusion that they will predict equal settlements provided $\nu = 0.363$. For $\nu < 0.363$, however, Boussinesq formula, Eq. [66], predicts slightly larger settlements than Lamé's formula, Eq. [67], while for $\nu > 0.363$, the settlements calculated from Lamé's formula become larger, up to a maximum of 27% at $\nu = 0.50$.

B. Solution for a $\phi > 0$ Material

Case (B-1): Nonlinear Creep Behavior

Stresses and Displacements in Prefailure Region. Since the behavior of the material in prefailure state is assumed to be given by Eq. [22] which is mathematically analogous to Eq. [15], the solution in the outer prefailure region around the cavity is identical to that in Case A, Eqs. [27]–[30], the only difference being that σ_s should now be replaced by σ_{sa} according to Eq. [23].

Stresses and Displacements in Failure Region. Following the same reasoning as in Case A, but using Eq. [24] as the failure condition, one gets a corresponding set of expressions for stresses and displacements in the failure region

around an expanding spherical cavity in a frictional frozen soil.

Stresses

$$[68] \quad \sigma_r = (p_i + H)\left(\frac{r_i}{r}\right)^{2(1-(1/f))} - H$$

$$[69] \quad \sigma_t = \frac{1}{f}(p_i + H)\left(\frac{r_i}{r}\right)^{2(1-(1/f))} - H$$

From the condition of continuity of stresses at the interface between the failure and non-failure regions, the extent of the failure region is

$$[70] \quad \frac{r_e}{r_i} = \left[\frac{(k-n)(p_i + H)}{k(p_o + H)}\right]^{f/2(f-1)}$$

where

$$[71] \quad k = \frac{3f}{2(f-1)} = \frac{3}{4}\left(\frac{1}{\sin\phi} + 1\right)$$

and the displacement at the interface

$$[72] \quad \frac{u_e}{r_e} = \frac{1}{2}\left[\frac{3(p_o + H)}{2\sigma_{sa}(k-n)}\right]^n$$

As in Case A, the displacement of the cavity wall can be determined from Eqs. [38] and [39]. After substituting Eqs. [70] and [72] into Eq. [39], the following is obtained:

$$[73] \quad A_s' = \left\{e_{av} + \frac{3}{2}\left[\frac{3(p_o + H)}{2\sigma_{sa}(k-n)}\right]^n\right\} \times \left\{\frac{(k-n)(p_i + H)}{k(p_o + H)}\right\}^k$$

The asymptotic expansion pressure, p_{ias}, is obtained by setting $A_s' = 1$, which yields

$$[74] \quad \frac{p_{ias} + H}{p_o + H} = N_p = \frac{k}{k-n} \times \left\{e_{av} + \frac{3}{2}\left[\frac{3(p_o + H)}{2\sigma_{sa}(k-n)}\right]^n\right\}^{-1/k}$$

If the right-hand side of Eq. [74] is called the 'cavity expansion factor' and denoted by N_p, Eq. [74] can be written as

$$[75] \quad p_{ias} = p_o N_p + H(N_p - 1)$$

The corresponding asymptotic punching pressure is then

$$[76] \quad q_{as} = p_o N_q + cN_c$$

where (for $\cot\alpha \approx 1$)

$$[77] \quad N_q = N_p(1 + \tan\phi)$$

and

$$[78] \quad N_c = (N_q - 1)\cot\phi$$

For graphical representation of typical values of the N_c factor, it has been found convenient to write the complete equation for N_q in the form (with e_{av} taken equal to zero):

$$[79] \quad N_q = (1 + \tan\phi)\left(\frac{2}{3}\right)^{1/k}(kI_r\tan\phi)^{n/k} \times (1 - n/k)^{(n/k-1)}$$

where I_r is a generalized 'rigidity index', analogous to that introduced by Vesić (1963) for the linear-elastic-plastic case of cavity expansion.[1] For the nonlinear-elastic-plastic incompressible case considered here, I_r is defined by

$$[80] \quad I_r = \frac{2\sigma_{sa}}{3(p_o + H)}\cot\phi$$

which can also be written as

$$[81] \quad I_r = \frac{2\sigma_{sa}}{3c}\left(1 + \frac{p_o}{c}\tan\phi\right)^{-1}$$

or

$$[82] \quad I_r = \frac{4\sqrt{f}}{3\epsilon_f^{1/n}}\left(1 + \frac{p_o}{c}\tan\phi\right)^{-1}$$

Figures 8–10 show the variation of the N_c factor with I_r for $n = 1$, 3, 5, and 7, and for several values of angle ϕ from $\phi = 0$ to ϕ_{max}, which is obtained at the limit of validity of the formula, *i.e.* for $k = n$.

For the $\phi = 0$ case, I_r becomes

$$[83] \quad I_r = 2\sigma_s/3c$$

so that, Eq. [46] can also be written as

$$[84] \quad N_{c(\phi=0)} = 1 + \tfrac{4}{3}[n + \ln\tfrac{2}{3}(\tfrac{3}{4}I_r)^n]$$

Pressure-settlement Behavior

Failure Region Exists. Inspecting Eq. [70] and taking into account Eq. [4] shows that the failure region will appear around the cavity as soon as

$$[85] \quad \frac{p_i + H}{p_o + H} = \frac{q + H}{p_o + H}(1 + \eta\tan\phi)^{-1} > \frac{k}{k-n}$$

[1] In a more recent publication, Vesić (1972) uses a new I_r which is exactly one half of the originally proposed I_r value.

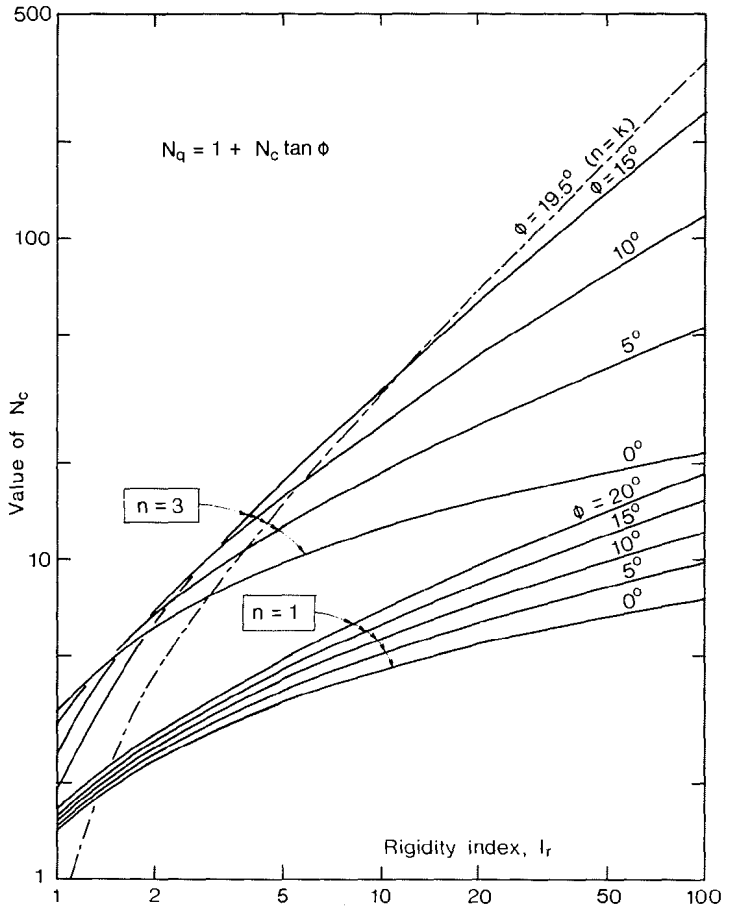

FIG. 8. Values of bearing capacity factor N_c for $\phi \geqslant 0$ and for $n = 1$ and 3.

which, obviously, is possible only if

$$k > n$$

If the above conditions are fulfilled, the isochronous settlement curve can be calculated as follows:
From Eq. [75]:

$$p_o + H = (p_{ias} + H)/N_p$$

so that

$$[86] \qquad \frac{p_i + H}{p_o + H} = \left(\frac{p_i + H}{p_{ias} + H}\right) N_p$$

On the other hand, dividing Eq. [4] by Eq. [11] (with $\alpha \approx 45°$)

$$[87] \qquad \frac{p_i + H}{p_{ias} + H} = R = \left(\frac{q + H}{q_{as} + H}\right)\left(\frac{1 + \tan \phi}{1 + \eta \tan \phi}\right)$$

Combining Eq. [87] with Eq. [86] shows that, in terms of punching pressure, the condition, Eq. [85], for the existence of failure region becomes:

$$[88] \qquad \frac{q + H}{q_{as} + H} > \left(\frac{1 + \eta \tan \phi}{1 + N_c \tan \phi}\right)\left(\frac{k}{k - n}\right)$$

When the failure region exists, Eqs. [38] and [73] are valid. Thus, proceeding similarly as in Case A when developing Eq. [52], one gets from Eqs. [38] and [73]:

$$[89] \qquad \frac{V_i}{V_{io}} = \frac{1 - e_{av}}{1 - R^k}$$

where R is given by the left-hand side of Eq. [87] for cavity expansion and by the right-hand side of Eq. [87] for the punching problem, or alternatively by

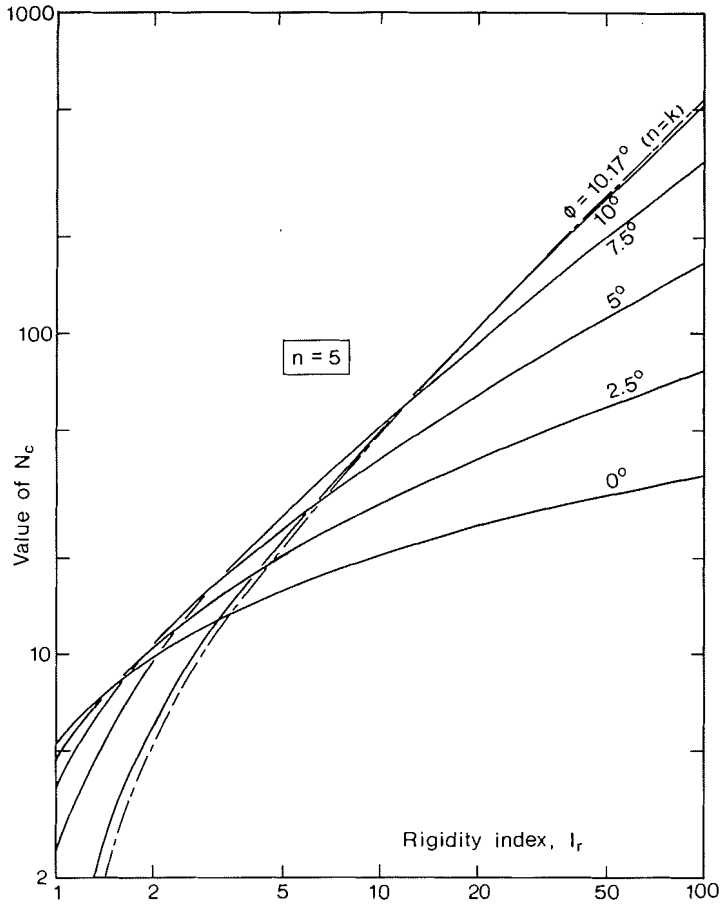

FIG. 9. Values of bearing capacity factor N_c for $\phi \geqslant 0$ and $n = 5$.

$$[90] \quad R = \left(\frac{q + H}{p_o + H}\right)\left(\frac{1 + \tan \phi}{1 + \eta \tan \phi}\right) \times (1 + N_c \tan \phi)$$

Taking Eq. [10] into account, the equation of an isochronous creep-settlement curve becomes:

$$[91] \quad \frac{s}{B} = \frac{1}{3}\left(\frac{V_i}{V_{io}} - 1\right) = \frac{R^k - e_{av}}{3(1 - R^k)}$$

In ice-rich frozen soils, the volume strain e_{av} may usually be neglected.

Failure Region does not Exist. According to Eq. [70], if either $k < n$, or

$$[92] \quad \frac{q + H}{p_o + H} < \frac{k}{k - n}(1 + \eta \tan \phi)$$

there will be no failure region around the expanding cavity for any pressure, and consequently no asymptotic expansion pressure.

However, the settlement can, nevertheless, be calculated from the nonlinear-creep theory as in Case A, by using Eq. [57] in which σ_s should be replaced by σ_{sa}, and $(p_i - p_o)$ by Eq. [4]:

$$[93] \quad p_i - p_o = \frac{q + H}{1 + \eta \tan \phi} - (p_o + H)$$

Obviously, at small loads ($q \ll q_{as}$) and, therefore, small settlement ($\eta \approx 0$), it is sufficiently accurate to take

$$[94] \quad p_i - p_o \approx q - p_o$$

Case (B-2): Linear Creep Behavior

Again, this case is a special case of the foregoing nonlinear case (B-1). In order to get the corresponding solution for the case (B-2), it is sufficient to take $n = 1$ and to replace σ_{sa} by the (time and temperature dependent) modulus of elasticity E. One gets then an incompressible version of the well known linear elastic per-

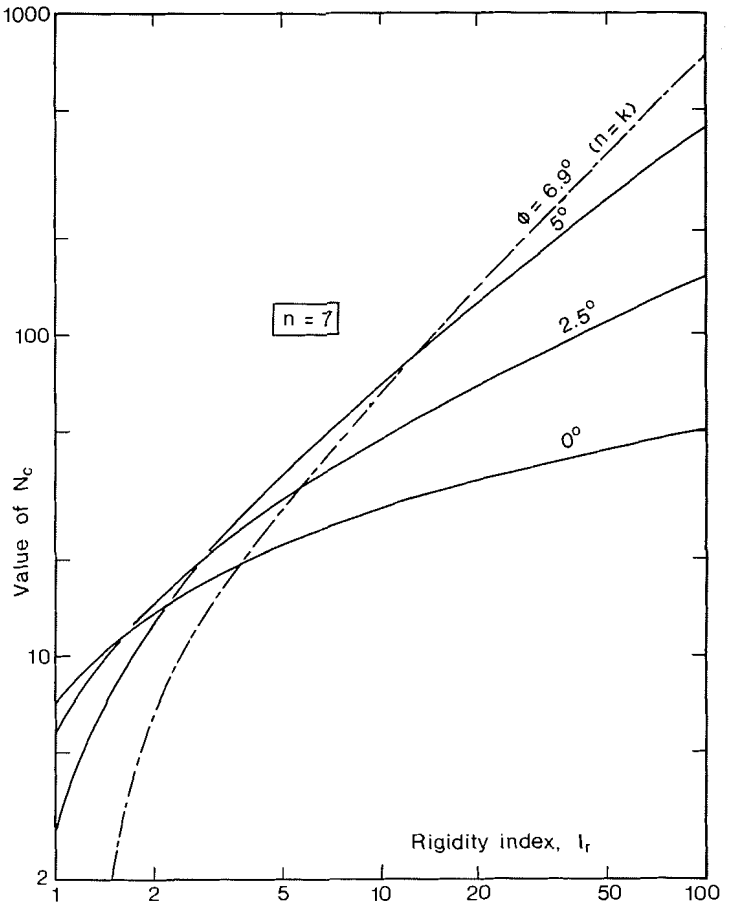

FIG. 10. Values of bearing capacity factor N_c for $\phi \geq 0$ and $n = 7$.

fectly plastic solution for an expanding spherical cavity in a frictional medium (Skempton *et al.* 1953; Vesić 1963).

Recapitulation

In order to facilitate the use of the proposed theory in the design of deep circular footings and anchors in permafrost, the most important formulae for the two nonlinear cases, A-1 and B-1, are recapitulated in the following.

Case A-1: $\phi = 0$ Material; Nonlinear Creep Behavior

Basic Soil Parameter

The time and temperature dependent cohesion, c, defined by

$$[19] \qquad c = \tfrac{1}{2}\sigma_{cu\theta}(\epsilon_f/\dot{\epsilon}_c t)^{1/n}$$

Asymptotic Punching Pressure

$$[45] \qquad q_{as} = p_o N_q + cN_c$$

where

$$N_q = 1$$

$$[46] \qquad N_c = 1 + \frac{4}{3}\left(n + \ln\frac{2}{3\epsilon_f}\right)$$

Some values of the N_c factor, for $1 \leq n \leq 10$ and $0.01 \leq \epsilon_f \leq 0.12$, are shown graphically in Fig. 7.

Isochronous Pressure-displacement Curves

If

$$[55] \qquad q - p_o < c(4n/3 + \eta)$$

there is no failure zone, and

$$[58] \qquad s/B = \frac{1}{3}\left\{\left[1 - \frac{\epsilon_f}{2}\left(\frac{3(q - p_o - \eta c)^n}{4nc}\right)\right]^{-3} - 1\right\}$$

If

[48] $$q - p_o > c(4n/3 + \eta)$$

the failure zone exists, and

[54] $$s/B = \frac{1}{3}\left\{\left[1 - \exp\frac{3}{4}\left(\frac{q - p_o}{c} + 1 - \eta - N_c\right)\right]^{-1} - 1\right\}$$

Time to Failure Under a Load q

[60] $$t_f = \frac{\epsilon_f}{\dot{\epsilon}_c}\left[\frac{\sigma_{cu\theta}N_c}{2(q - p_o)}\right]^n$$

Case B-1: $\phi > 0$ Material; Nonlinear Creep Behavior

Basic Soil Parameters

The angle of internal friction ϕ and the time and temperature dependent cohesion, c, defined by

[102] $$c = \frac{\sigma_{cu\theta}}{2\sqrt{f}}\left(\frac{\epsilon_f}{\dot{\epsilon}_c t}\right)^{1/n}$$

where

[21] $$f = (1 + \sin\phi)/(1 - \sin\phi)$$

Additional, deduced, parameters:

[25] $$H = c\cot\phi$$

[71] $$k = 3f/2(f - 1)$$

[82] $$I_r = \frac{4\sqrt{f}}{3\epsilon_f^{1/n}}\left(1 + \frac{p_o}{c}\tan\phi\right)^{-1}$$

Asymptotic Punching Pressure

[76] $$q_{as} = p_o N_q + cN_c$$

where (for $e_{av} = 0$),

[79] $$N_q = (1 + \tan\phi)(\tfrac{2}{3})^{1/k}(kI_r\tan\phi)^{n/k} \times (1 - n/k)^{(n/k-1)}$$

[78] $$N_c = (N_q - 1)\cot\phi$$

Some values of the N_c factor, for $1 \leq I_r \leq 100$ and $n = 1, 3, 5$, and 7, are shown graphically in Figs. 8, 9, and 10.

Isochronous Pressure-displacement Curves

If either $k < n$, or

[92] $$\frac{q + H}{p_o + H} < \frac{k}{k - n}(1 + \eta\tan\phi)$$

there is no failure zone, and the creep displacements should be calculated by using Eq. (57), in which σ_s should be replaced by σ_{sa}, defined by

[23] $$\sigma_{sa} = [\sigma_{cu\theta} + \sigma_{3av}(f_c - 1)](\dot{\epsilon}_c t)^{-1/n}$$

and $(p_i - p_o)$ by

[93] $$p_i - p_o = \frac{q + H}{1 + \eta\tan\phi} - (p_o + H)$$

If both $k > n$ and

[85] $$\frac{q + H}{p_o + H} > \frac{k}{k - n}(1 + \eta\tan\phi)$$

the failure zone exists, and

[91] $$s/B = \frac{R^k - e_{av}}{3(1 - R^k)}$$

where

[90] $$R = \left(\frac{q + H}{p_o + H}\right)\left(\frac{1 + tan\,\phi}{1 + \eta\tan\phi}\right)N_q$$

NOTE: In all these expressions, $\sigma_{cu\theta} = \sigma_{cuo}f(\theta)$, denotes the creep modulus of the frozen soil, which is equal to the uniaxial (unconfined) compression strength of the soil at a temperature of θ degrees Celsius below 0 °C, and at a strain rate $\dot{\epsilon}_1^{(c)} = \dot{\epsilon}_c$. The values of $\sigma_{cu\theta}$, n, ϕ, and ϵ_f have to be determined experimentally, either by means of laboratory tests, as described in Ladanyi (1972), or by using a field technique, such as the one shown by Ladanyi and Johnston (1973).

Comparison of Theoretical Predictions with Experimental Results

The theory proposed in this paper is well suited for predicting the behavior, under a pull load, of deep circular anchor plates embedded in permafrost. In fact, an extensive study of such anchors under long term loading was carried out between 1967 and 1970 by the Division of Building Research of the National Research Council at Thompson, Manitoba. The study was followed in 1971 by a thorough investigation of creep and time dependent strength properties of the frozen soil at the same site by means of specially designed pressuremeter tests.

A detailed description of the screw anchor tests is given in the paper by Johnston and Ladanyi (1974), while some typical pressuremeter test results obtained at the site have been presented in a paper by Ladanyi and Johnston (1973).

A detailed description of the site and soil conditions was given in a recent paper by

Johnston and Ladanyi (1972), describing grouted rod anchor tests that were performed at the site during the same period of time. Consequently, only some basic information necessary for understanding the comparison need be repeated here.

Soil Conditions at the Test Site

Within the depth interval investigated, *i.e.* between 5 and 14 ft (1.50 and 4.20 m), the soil was a varved clay of low to medium plasticity, composed of dark brown clay layers from 0.5 to 1.0 in. (12 to 25 mm) thick, and tan-colored silt layers increasing in thickness with depth from 1.0 to 3.0 in. (25 to 75 mm).

The most significant ice segregation was found in the top 13 ft (4.20 m) and was usually associated with the dark layers. Ice lenses were mainly horizontal and varied in thickness from hairline to a maximum of about 0.5 in. (12 mm). Permafrost temperatures at depths between 5 and 30 ft (1.50 and 9.00 m), were fairly uniform, varying between 31.5 and 31.8 °F (−0.10 and −0.30 °C) throughout the year.

Some Typical Results of Screw Anchor Tests

A total of 12 screw anchors were installed at the site in 1967. These were tested during 1969 and 1970. Ten of the screw anchors had single helices ranging in diameter from 8 to 15 in. (20 to 38 cm). The anchors were installed at depths varying from 8 to 14 ft (2.40 to 4.20 m). The other two were double helix anchors.

Three typical tests on anchors 1-1ON, 2-1ON, and 1-1OHP have been selected for comparison purposes. The three were single helix anchors having a diameter $B = 10$ in. (25.4 cm), and were installed at depth, D, of 9 to 10 ft (2.70 to 3.00 m). All were stage loaded to failure in 7–8 stages, giving an average total test duration of about 40 h.

In order to put the test results in a more general form, the data were treated in a manner similar to that proposed by Hult (1966) and Ladanyi (1972) for generalizing the steady-state creep data. In other words, for each stage, the pseudo-instantaneous displacement and the steady-state creep rate were determined and plotted against the applied load.

As expected, the resulting creep and displacement functions were both of a hyperbolic type. In particular, for steady-state creep rates, the following form was found convenient (Johnston and Ladanyi 1974):

$$[95] \qquad \dot{s} = \dot{s}_c \bar{C} \frac{q_{net} + \gamma D}{q_{as,net} - q_{net}}$$

where $\dot{s}$ is the displacement rate in in./min, $\dot{s}_c$ is an arbitrary displacement rate, $\bar{C}$ is and experimental dimensionless parameter, and q_{net} is the net pressure defined by

$$[96] \qquad q_{net} = q - \gamma D$$

q denoting the total applied pressure. Numerical data for the depth D, the overburden pressure γD, the parameter $\bar{C}$, the asymptotic ultimate pressure $q_{as,net}$, and the time to failure for the three anchor tests, are given in Table 1 (Johnston and Ladanyi 1974).

Figure 11 shows for the three tests, according to this generalized information, the creep rates *versus* q_{net} plot and the value of the average ultimate pressure, $q_{as,net} = 201$ p.s.i. (14.1 kg/cm^2). The value of $q_{as,net}$, which corresponds to an infinite displacement rate is, obviously, the ultimate pull-out resistance of the anchors.

In order to compare the observed behavior of the anchors with theoretical predictions, use was made of frozen soil creep information obtained by pressuremeter tests described in Ladanyi and Johnston (1973). In that paper, it was shown that the results of stage-loaded pressuremeter creep tests could be expressed by a creep law of the form

$$[97] \qquad \epsilon_e^{(c)} = (\dot{\epsilon}_c'/b)^b (\sigma_e/\sigma_c)^n t^b$$

where $\epsilon_e^{(c)}$ and σ_e are equivalent creep strain and equivalent stress respectively, b, n, and σ_c are material constants for a given temperature, and $\dot{\epsilon}_c'$ is an arbitrary strain rate. A pressuremeter test being of relatively a short duration, Eq. [97] is of the primary creep type (*i.e.* $b < 1$). When extrapolating this kind of data to long term creep processes, it is more convenient, and on the safe side, to transform the data to a steady-state creep, by assuming that the creep rate remains constant after a given period of primary creep. In order to do that, it is only necessary to differentiate Eq. [97] with respect to t and to put $t = t_o = \text{const}$. This gives

$$[97a] \qquad \dot{\epsilon}_c^{(c)} = b(\dot{\epsilon}_c'/b)^b t_o^{b-1} (\sigma_e/\sigma_c)^n = \dot{\epsilon}_c (\sigma_e/\sigma_c)^n$$

For the two pressuremeter tests, numbers 9-1 and 10-1, used for the comparison, the

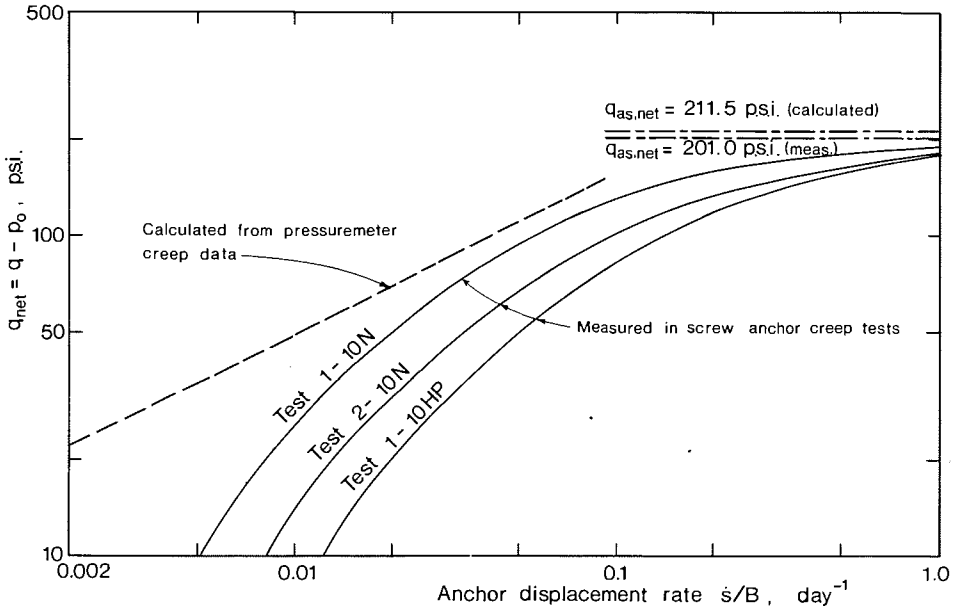

FIG. 11. Comparison of measured and calculated displacement rates and failure loads for deep screw anchors in permafrost.

TABLE 1. Numerical data for the three anchor tests

Anchor No.	Diameter B (in.)	Depth D (ft)	γD (p.s.i.)	$\dot{S}_c$ (in./min)	$\bar{C}$	$q_{as,act}$ (p.s.i.)	Time to failure (h)
1-10N	10	10.0	8.67	10^{-5}	36.7	203.8	72
2-10N	10	9.3	8.06	10^{-5}	57.7	192.0	23
1-10HP	10	9.0	7.80	10^{-5}	92.0	202.2	22

following average values of the parameters were obtained: $n = 2.095$, $b = 0.633$, $\sigma_c = 69$ p.s.i. (4.8 kg/cm^2), for $\dot{\epsilon}_c' = 10^{-5}$ min^{-1}.

Since it was found that the creep curves in anchor tests became linear after about 2 h, $t_o = 120$ min was adopted, and the following creep rate equation was deduced from Eq. [99]

$$[99] \qquad \dot{\epsilon}_c^{(c)} = 10^{-4}(\sigma_c/69)^{2.095} \text{ min}^{-1}$$

Sufficient information is, therefore, available to complete Eq. [61], since from Eq. [99] $\dot{\epsilon}_c = 10^{-4}$ min^{-1} = 0.144 day^{-1}, $\sigma_{cu\theta} = 69$ p.s.i. (4.8 kg/cm^2) (for the same temperature) and $n = 2.095$. Therefore,

$$[100] \qquad \dot{u}_i/r_i = 0.072 \left(\frac{p_i - p_o}{96.37}\right)^{2.095} \text{ day}^{-1}$$

with $(p_i - p_o)$ in pounds per square inch. The corresponding displacement rate $\dot{s}/B$ was then obtained by substituting $\dot{u}_i/r_i$ into Eq. [56] and by taking into account that, according to Eq. [4], for a given $p_i - p_o$, the corresponding net pressure is given by

$$[101] \qquad q - p_o = (p_i - p_o)(1 + \eta \tan \phi) + (p_o + H)\eta \tan \phi$$

In the calculation, η was taken to vary linearly from 0 at $q - p_o = 0$ to 1.0 at $q - p_o =$ 100 p.s.i. (7 kg/cm^2) at which $s/B \approx 0.10$ was attained in the tests.

In order to be able to determine the value of H, the long term strength of the soil should be known. The cohesion, c, corresponding to the average time to failure $t_f = 40$ h = 2400 min in the three anchor tests, was calculated from the formula (Eqs. [19] and [26])

$$[102] \qquad c = \frac{\sigma_{cu\theta}}{2\sqrt{f}} \left(\frac{\epsilon_f}{t\dot{\epsilon}_c}\right)^{1/n}$$

For frozen varved silt-clay, an angle of friction of $\phi = 15°$ may be assumed, while a failure strain of $\epsilon_f = 0.10$ was observed on stress–strain curves in pressuremeter tests.

This yields

$$c = \frac{69}{2\sqrt{1.695}}\left(\frac{0.10}{2400 \times 10^{-4}}\right)^{0.4773} =$$

17.45 p.s.i. (1.22 kg/cm^2)

and

$$H = c \cot \phi = 17.45 \times 3.732$$

$$= 65.12 \text{ p.s.i. } (4.56 \text{ kg/cm}^2)$$

The resulting displacement rate *versus* q_{net} relationship is shown dashed in Fig. 11. Since the case without failure zone was assumed in the calculation, the validity of this line extends only to about 145 p.s.i. (10.2 kg/cm^2), according to Eq. [92].

In order to determine the asymptotic ultimate pull-out resistance, the value of I_r should first be calculated from Eq. [82]. For $p_o = \gamma D =$ 8.67 p.s.i. (0.6 kg/cm^2), one gets: $I_r = 4.596$. Since $k = 3.658$ (Eq. [71]), one gets $N_p = 3.049$ (Eq. [74]), $N_q = 3.866$ (Eq. [77]) and $N_c = 10.70$ (Eq. [78]). The N_c value can also be obtained by interpolation from Fig. 8. The asymptotic pressure is then, by Eq. [76], $q_{as} = 220.17$ p.s.i. (15.41 kg/cm^2), and $q_{as,net} = 211.50$ p.s.i. (15.11 kg/cm^2).

The last value has been plotted in Fig. 11 and is seen to agree very well with the average ultimate pulling resistance of the three anchors, $q_{as,net} = 201$ p.s.i. (14 kg/cm^2).

When comparing the observed and the predicted behavior of the anchors, it is seen that the results obtained by substituting the pressuremeter data into the theory, come close to, but slightly underestimate the creep rates and overestimate the ultimate strength of the anchors. This is thought to be due to the fact that the soil above the anchors has been disturbed by their installation and may therefore be expected to be slightly weaker than the natural soil tested by the pressuremeter.

Conclusions

A method for predicting the creep settlement and the time dependent bearing capacity of frozen soils under deep circular loads has been developed and compared with available experimental information. The proposed solution takes into account the nonlinear viscoelastic character of the frozen soil, as well as the fact that its strength is a function of the time, the temperature and the normal pressure. The theory is intended primarily to provide all necessary design information for deep footings embedded in permafrost, but it can also be used for predicting the deviatoric nonlinear elastic and plastic settlement of footings in ordinary soils with negligible volume strains.

The predictive capacity of the theory was checked against the results of screw anchor tests carried out at a permafrost site in Thompson, Manitoba. It was found that the use in the theory of pressuremeter-determined creep parameters of the frozen soil at the site, resulted in satisfactory agreement between the predicted and the observed behavior of three typical anchors.

Acknowledgments

This work was initiated during the first author's 1970 summer term as a visiting professor at the Division of Building Research, National Research Council of Canada, Ottawa, Canada.

The authors wish to acknowledge the constructive discussions and criticisms by members of the Geotechnical Section, especially Dr. L. W. Gold, Head of the Section, who made a number of helpful suggestions for improving the manuscript.

ALKIRE, B. D., and ANDERSLAND, O. B. 1973. The effect of confining pressure on the mechanical properties of sand-ice materials. J. Glaciol. **12**(66), pp. 469–481.

ANDERSLAND, O. B., and ALNOURI, I. 1970. Time dependent strength behavior of frozen soils. Proc. A.S.C.E. **96**(SM4), pp. 1249–1265.

BEREZANTSEV, V. G. 1956. Bearing capacity of foundations at an axially symmetric state of stress. (*In Russian.*) Proc. Conf. Soil Mech. Found. Eng., Gostroyizdat, Moscow, U.S.S.R. pp. 84–88.

BISHOP, R. F., HILL, R., and MOTT, N. F. 1945. The theory of indentation and hardness tests. Proc. Phys. Soc., Lond. **57**(3), pp. 147–159.

BURLAND, J. B., BUTLER, F. G., and DUNICAN, P. 1966. The behavior and design of large diameter bored piles in stiff clay. Proc. Symp. Large Bored Piles, London, Engl. pp. 51–71.

DE BEER, E. E., and LADANYI, B. 1961. Etude expérimentale de la capacité portante du sable sous des fondations circulaires établies en surface. Proc. 5th Int. Conf. Soil Mech. Found. Eng., Paris, France. **1**, pp. 577–585.

DUGDALE, D. S. 1958. Vickers hardness and compressive strength. J. Mech. Phys. Solids. **6**, pp. 85–91.

DUNCAN, J. M., and CHANG, C. Y. 1970. Nonlinear

analysis of stress and strain in soils. Proc. A.S.C.E. 96(SM5), pp. 1629–1635.

GIBSON, R. E. 1950. Discussion. J. Inst. Civ. Eng. **34**, p. 382.

GILL, D. E. 1970. A mathematical model for lining design in linear viscoelastic ground. Ph.D. thesis, McGill Univ., Montreal, Quebec.

GIRIJAVALLABHAN, C. V., and REESE, L. C. 1968. Finite-element method for problems in soil mechanics. Proc. A.S.C.E. 94(SM2), pp. 473–496.

HILL, R. 1950. The mathematical theory of plasticity. Clarendon Press, Oxford, Engl.

HIRST, W., and HOWSE, M. G. J. W. 1969. The indentation of materials by wedges. Proc. Phys. Soc. **A311**, pp. 429–444.

HOFF, N. J. 1954. Approximate analysis of structures in the presence of moderately large creep deformations. Q. Appl. Math. **12**, pp. 49–55.

HULT, J. A. H. 1966. Creep in engineering structures. Blaisdell Publ. Co., Waltham, Mass.

JOHNSON, K. E. 1970. The correlation of indentation experiments. J. Mech. Phys. Solids. **18**, pp. 118–126.

JOHNSTON, G. H., and LADANYI, B. 1972. Field tests of grouted rod anchors in permafrost. Can. Geotech. J. 9, pp. 176–194.

——— 1974. Field tests of deep power-installed screw anchors in permafrost. Can. Geotech. J. **11**, pp. 348–358.

LADANYI, B. 1959. Etude théorique et expérimentale du problème de l'expansion dans un sol pulvérulent d'une cavité présentant une symétrie sphérique ou cylindrique. Ph.D. thesis, Univ. Louvain, Louvain, Belg.

——— 1963. Evaluation of pressuremeter tests in granular soils. Proc. 2nd Panam. Conf. Soil Mech. Found. Eng., Sao Paulo. Braz. **1**, pp. 3–20.

——— 1966. Failure mechanism of rock under a plate load. Proc. First Cong. Int. Soc. Rock Mech., Lisbon, Port. **1**, pp. 415–420.

——— 1967a. Deep punching of sensitive clays. Proc. 3rd Panam. Conf. Soil Mech. Found. Eng., Caracas, Venez. **1**, pp. 535–546.

——— 1967b. Expansion of cavities in brittle media. Int. J. Rock Mech. Min. Sci. **4**, pp. 301–328.

——— 1972. An engineering theory of creep of frozen soils. Can. Geotech. J. **9**, pp. 63–80.

LADANYI, B., and JOHNSTON, G. H. 1973. Evaluation of in-situ creep properties of frozen soils with the pressuremeter. Proc. 2nd Int. Conf. Permafrost, Yakutsk, U.S.S.R. North Am. Contrib., pp. 310–318.

MARSH, D. M. 1964. Plastic flow of glass. Proc. R. Soc., Lond. **279A**, pp. 420–435.

MEYERHOF, G. G. 1963. Some recent research on the bearing capacity of foundations. Can. Geotech. J. **1**, pp. 15–26.

MEYERHOF, G. G., and ADAMS, J. I. 1968. The ultimate uplift capacity of foundations. Can. Geotech. J. **5**, pp. 225–244.

MULHEARN, T. O. 1959. The deformation of metals by Vickers-type pyramidal indenters. J. Mech. Phys. Solids, **7**, pp. 85–96.

ODQUIST, F. K. G., and HULT, J. 1962. Creep in metallic materials (*in German*). Springer, Berlin, Germ.

SAYLES, F. H. 1973. Triaxial and creep tests on frozen Ottawa sand. Proc. 2nd Int. Conf. Permafrost, Yakutsk, U.S.S.R. North Am. Contrib., pp. 384–391.

SKEMPTON, A. W., YASSIN, A. A., and GIBSON, R. E. 1953. Théorie de la force portante des pieux dans le sable. Annls. Inst. Tech. Bat. Trav. Publ. **63/64**, pp. 285–289.

VESIĆ, A. S. 1963. Theoretical studies of cratering mechanisms affecting the stability of cratered slopes. Rep. Soil. Mech. Lab., Georgia Inst. Tech., Atlanta, Ga.

——— 1972. Expansion of cavities in infinite soil mass. Proc. A.S.C.E. **98**(SM3), pp. 265–290.

VIALOV, S. S. 1959. Rheological properties and bearing capacity of frozen soils. Transl. 74, U.S. Army C.R.R.E.L., Hanover, N.H., 1965.

Appendix – Symbols

A_s, A_s' = factors defined by Eqs. [40] and [73]
b = exponent in creep equation
B = footing diameter
c = cohesion intercept
D = footing depth
e_{av} = average volume strain in the plastic zone
E = Young's modulus
f = flow value, Eq. [21]
H = $c \cot \phi$
I_r = rigidity index, Eqs. [80]–[82]
k = $F(\phi)$, Eq. [71]
n = exponent in creep equation
N_c, N_q = bearing capacity factors
N_{pc}, N_p = ultimate cavity expansion factors
p_i = cavity expansion pressure
p_{ias} = ultimate (asymptotic) cavity expansion pressure
p_o = average total original ground stress at the footing level
q = applied pressure on the footing
q_{as} = ultimate resistance (bearing capacity) of the footing
r = radius
r_i = current radius of the cavity
r_{io} = initial radius of the cavity
r_e = current radius of failure zone
R = ratio, Eq. [90]
s = settlement or displacement
t = time
u = radial displacement
V_i = current cavity volume
V_{io} = initial cavity volume
Y = yield stress
α = semi-angle of the rigid soil cone moving with the footing
γ = total unit weight of frozen soil

$\epsilon^{(c)}$ = creep strain
$\dot{\epsilon}_c$ = arbitrary strain rate in creep equation
ϵ_f = creep failure strain
ϵ_r, ϵ_t = radial and circumferential principal strains
θ = number of degrees Celsius below 0 °C
η = degree of mobilization of friction on the cone
ν = Poisson's ratio
σ_c = proof stress (creep modulus) in creep equation
$\bar{\sigma}_c$ = creep modulus, Eq. [13]
σ_{ca} = σ_c, average value for creep in uniaxial compression
σ_{cu} = σ_c for creep in uniaxial compression
σ_{cuo} = σ_{cu} at freezing temperature close to 0 °C
$\sigma_{cu\theta}$ = $\sigma_{cu} f(\theta) = \sigma_{cu}$ at freezing temperature θ
σ_{fu} = creep failure stress in uniaxial compression
σ_1, σ_3 = major and minor principal stress
σ_r, σ_t = radial and tangential principal stress around the cavity
σ_{re} = radial stress at the boundary of the failure zone
σ_s = creep modulus, Eq. [16]
$\sigma_{s:t}$ = creep modulus, Eq. [23], for an average confining pressure, σ_{3av}
ϕ = angle of internal friction

NOTE: dot over symbols denotes time rate.